Non-CpG methylation by DNMT3B facilitates REST binding and gene silencing in developing mouse hearts

Donghong Zhang[1], Bingruo Wu[1], Ping Wang[2], Yidong Wang[1], Pengfei Lu[1], Tamilla Nechiporuk[3], Thomas Floss[4], John M. Greally[5], Deyou Zheng[6,*] and Bin Zhou[1,7,*]

[1]Departments of Genetics, Pediatrics, and Medicine (Cardiology), Wilf Cardiovascular Research Institute, Albert Einstein College of Medicine, Bronx, NY 10461, USA, [2]Department of Neurology, Albert Einstein College of Medicine, Bronx, NY 10461, USA, [3]Vollum Institute, Oregon Health & Science University, Portland, OR 97239, USA, [4]German Research Center for Environmental Health, Neuherberg, Germany, [5]Departments of Genetics, Medicine (Hematology), and Pediatrics, Albert Einstein College of Medicine, Bronx, NY 10461, USA, [6]Departments of Genetics, Neurology, and Neuroscience, Albert Einstein College of Medicine, Bronx, NY 10461, USA and [7]Department of Cardiology, The First Affiliated Hospital of Nanjing Medical University, Nanjing, China

ABSTRACT

The dynamic interaction of DNA methylation and transcription factor binding in regulating spatiotemporal gene expression is essential for embryogenesis, but the underlying mechanisms remain understudied. In this study, using mouse models and integration of *in vitro* and *in vivo* genetic and epigenetic analyses, we show that the binding of REST (repressor element 1 (RE1) silencing transcription factor; also known as NRSF) to its cognate RE1 sequences is temporally regulated by non-CpG methylation. This process is dependent on DNA methyltransferase 3B (DNMT3B) and leads to suppression of adult cardiac genes in developing hearts. We demonstrate that DNMT3B preferentially mediates non-CpG methylation of REST-targeted genes in the developing heart. Downregulation of DNMT3B results in decreased non-CpG methylation of RE1 sequences, reduced REST occupancy, and consequently release of the transcription suppression during later cardiac development. Together, these findings reveal a critical gene silencing mechanism in developing mammalian hearts that is regulated by the dynamic interaction of DNMT3B-mediated non-CpG methylation and REST binding.

INTRODUCTION

Heart development is regulated by a complex program involving transcriptional and epigenetic processes. A dysregulated cardiac gene program impairs cardiogenesis and cardiac function, leading to cardiac hypertrophy, arrhythmia and heart failure (1,2). Repressor element 1 (RE1)-silencing transcription factor (REST; also known as NRSF for Neuron Restrictive Silencer Factor) is known to suppress the expression of neuronal genes in non-neuronal cells (3,4), but its functions have been recently shown to be more diverse. In developing mouse hearts, REST represses the expression of a subset of cardiac genes, such as atrial natriuretic peptide (*Nppa*), brain natriuretic peptide (*Nppb*), and the pacemaker hyperpolarization-activated cyclic nucleotide-modulated potassium channel protein 2 (*Hcn2*) (5,6). Developmentally regulated expression of *Hcn2*, which encodes the prominent HCN isoform expressed in the adult ventricular cardiomyocytes, contributes to the maturation of cardiac pacemaker channels (7–9). While critically important in the development of rhythmic heartbeat, the mechanism underlying the repression of *Hcn2* and other cardiac genes by REST during heart development is poorly understood.

It has been previously shown that REST represses its targets mainly through the recruitment of a cohort of chromatin modifiers, such as histone deacetylases (HDACs), including the SIN3 complex, and methyl-binding proteins such as methyl-CpG binding protein 2 (Mecp2) (10,11). In non-neuronal cells, REST strongly represses gene expression when its binding sites, the Repressor Element 1 (RE1) motifs, have more CpG DNA methylation (10,12). Our previous genome-wide study has also shown that DNA methylation of the cardiac-essential genes is developmentally regulated, a process involving *de novo* DNA methyltransferase 3B (DNMT3B) (13). In addition, abnormal DNA methylation during development has been associated with cardiac

---

*To whom correspondence should be addressed. Tel: +1 718 678 1067; Fax: +1 718 678 1016; Email: deyou.zheng@einstein.yu.edu
Correspondence may also be addressed to Bin Zhou. Tel: +1 718 678 1067; Fax: +1 718 678 1016; Email: bin.zhou@einstein.yu.edu

hypertrophy (14,15). It is therefore interesting to investigate how REST function is related to DNA methylation during heart development.

The majority of cytosine methylation in mammalian genomes occurs at CpG dinucleotides, with non-CpG (CpA, CpT and CpC) dinucleotides generally accounting for a relatively small proportion of total cytosine methylation. Recent studies have, however, shown that non-CpG methylation is high in pluripotent stem cells and several other cell types (such as oocytes) (16–22). In particular, non-CpG methylation (e.g. CpAs) is found to be the major form of DNA methylation in human neurons (23–25) and is important for gene regulation (25–28). Whether non-CpG methylation plays a role in cardiac gene program during development is, however, currently unknown.

The consensus, 21-nt long, RE1 motif contains one CpG and 7 to 8 non-CpGs, and thus serves as a good model for addressing the potential roles of non-CpG methylation in the context of REST binding and gene suppression. In this study, we began by investigating DNA methylation at the *Hcn2* intronic RE1 (referred as *Hcn2*-RE1) in the developing mouse heart. Our results show that its non-CpG hypermethylation is dependent on DNMT3B and crucial for REST binding to suppress *Hcn2* transcription in early embryonic hearts. Extending the analysis genome-wide, we demonstrated that such a mechanism regulates the expression of >30% of REST-targeted genes in the developing heart. Taken together, the results of our study support a new mode of adult gene silencing in the developing heart that is mediated by the interaction between REST and non-CpG methylation, which in turn is regulated by DNMT3B.

MATERIALS AND METHODS

Experimental mice

Mouse experiments were carried out following the Guide for the Care and Use of Laboratory Animals published by NIH and the guidelines of the Institutional Animal Care and Use Committee (IACUC) of Albert Einstein College of Medicine. C57BL6 floxed *Dnmt3a* (*Dnmt3a*f/f) and *Dnmt3b* (*Dnmt3b*f/f) mice (29) were obtained from the Jackson Laboratory (Bar Harbor, Maine). C57BL/6 conditional gene trap (GT) cassette in an intron of the endogenous Rest gene *Rest (Rest*GT/GT*)* mice were generated at the Wellcome Trust Sanger Institute (Hinxton, UK) and described previously (30). C57/BL6 cardiac *Troponin T* Cre (*Tnnt*Cre) mice (31) were used for myocardial deletion of *Dnmt3a, Dnmt3b* or *Rest*. Conditional knockout (KO) mice were genotyped by PCR for Cre- and allele-specific primers. CD-1 wild-type mice were purchased from the Charles River Laboratories (Kinston, NY). Noontime on the day of observation of vaginal plugs was designated as embryonic day (E) 0.5. Pregnant mice were sacrificed at differential developmental stages, E10.5, E14.5, E18.5, postnatal (P) 1 and P21, by isoflurane inhalation. Ventricles were excised from isolated embryonic and postnatal hearts and immediately snap-frozen and stored in liquid nitrogen, as described before (13).

Primary neonate cardiomyocyte and cardiac fibroblast cultures

Primary neonate cardiomyocyte and cardiac fibroblast were isolated and cultured as described previously (32). In brief, ventricles were excised from P1 neonates and digested with 0.045% collagenase II and 0.08% trypsin–EDTA. Cardiomyocytes and cardiac fibroblast cells were separated by their differential adherence to the culture dish, and then maintained at 37°C and under 5% CO_2 in Dulbecco's modified Eagle's minimum essential medium (DMEM) supplemented with 10% fetal calf serum.

Quantitative reverse transcription PCR (qRT-PCR)

Total RNA was isolated from the ventricles using the Trizol Reagent. The first-strand cDNA was synthesized by incubation of 0.5 mg of total RNA with oligo dT and reverse transcriptase (Superscript III, Invitrogen), according to the manufacturer's protocol. qPCR was performed using the Power SYBR Green PCR Master Mix (Life Technologies) on the Applied Biosystems 7900HT Fast Real-Time PCR System (Thermo Fisher Scientific, MA). Primers are listed in Supplementary Table S1. The expression of *Gapdh* was used as an internal control for normalization. Relative changes in expression levels were calculated using the $2^{-\Delta\Delta}$CT method. All qRT-PCR analyses were performed in biological triplicates for each sample and student t-test was used for determining significance.

Western blot analysis

Protein lysates were extracted from ventricles for immunoblotting as previously described (33). Briefly, protein lysates were separated and incubated with primary antibodies against HCN2 (Proteintech, 555245-1-AP, 1:300 dilution), DNMT1 (Abcam, ab13537, 1:1000 dilution), DNMT3A (Abcam, ab13888, 1:1000 dilution), DNMT3B (Abcam, ab13604, 1:1000 dilution), REST (Antibodiesonline, ABIN747683, 1:1000 dilution), and GAPDH (Thermo Fisher Scientific, MA5-15738, 1:2000 dilution), overnight at 4°C, followed by the use of horseradish peroxidase (HRP)-conjugated secondary antibodies (1:1000 dilution), with subsequent detection using the Pierce™ ECL substrate with optimal exposure time for each antibody detection. The signal densities of protein bands were quantified and normalized to that of GAPDH using the ImageJ software (National Institutes of Health).

Bisulfite sequencing

Genomic DNA was extracted from the ventricles of embryos at different developmental stages, and modified by the BisulFlash DNA Modification kit (34). CpGenome Universal Unmethylated DNA (sigma, S7822-M) and Methylated Control DNA (Sigma, M8570) were used as positive and negative controls, respectively. PCR primers for detecting the *Hcn2-RE1* are listed in Supplementary Table S1. PCR fragments were gel purified using the MinElute Gel Extraction Kit and then cloned into the pCR2.1® vector. After bacterial transformation, 6–10 positive colonies were randomly selected for bisulfite sequencing. The percentage of

non-CpG methylation of each clone was calculated by the ratio of methylated sites to the total of non-CpG sites (for *Hcn2-RE1,* non CpG = 7). The average percentage of non-CpG methylation for the *RE1* was then calculated from the triplicate assays.

Chromatin immunoprecipitation (ChIP), quantitative ChIP (qChIP) and re-ChIP assays

30–50 mg of embryonic ventricles were minced, treated with formaldehyde, sonicated into 100–300 bp DNA fragments and immunoprecipitated using the magnet bead-bound antibodies (5 µg) against DNMT3A (Abcam, ab13888), DNMT3B (Abcam, ab13604) and REST (EMD Millipore, 17-641) or control IgGs (Abcam, ab171870). Immunoprecipitates were washed and eluted with elution buffers. The eluates were incubated at 65°C overnight to reverse the cross-links and then treated with RNase A, and followed by proteinase K treatment. The samples were purified using a PCR purification kit. In re-ChIP (sequential ChIP) experiments, the initial immunoprecipitated complexes were eluted by incubation with 10 mM dithiothreitol (DTT) at 37°C for 30 min, diluted 1:50 in the immunoprecipitation buffer, and re-immunoprecipitated with secondary antibodies or control IgG overnight at 4°C as previously described (35). Bound DNAs were extracted and used for PCR analysis to determine the enrichment of DNA fragments containing the *Hcn2-RE1,* using specific primers (Supplementary Table S1).

Luciferase reporter gene assay

The mouse *Hcn2* gene with or without the *Hcn2-RE1* was PCR cloned into the PGL3-enhancer luciferase reporter vector at KpnI and NheI (or Xho1). PCR primers for detecting the *Hcn2-RE1* are listed in Supplementary Table S1. All constructs were confirmed by Sanger sequencing. *Rest* siRNAs were purchased from the Einstein shRNA Core Facility, pcDNA/Myc-DNMT3A and cDNA/Myc-DNMT3B were obtained from Addgene (36). Lipofectamine LTX and PLUS Reagents (Life Technologies) were used for the transfection of siRNAs or the pcDNA3 expression constructs into the primary cultured ventricular cardiomyocytes. The efficiency of gene knockdown or over-expression of *Rest, Dnmt3a and Dnmt3b* was confirmed by immunofluorescence staining. The Renilla luciferase vector was co-transfected and used for normalizing transfection efficiency using the dual-luciferase reporter assay kit (Promega, E1980) according to the manufacturer's instructions. All data were normalized by Renilla luciferase luminescence derived from the co-transfected pRL-SV40 vector (Promega, E2231).

Electrophoretic mobility shift assay (EMSA)

An EMSA kit (Thermos Scientific, 20148) was used to detect REST binding to the *Hcn2-RE1* using nuclear extracts kit (Thermos Scientific, 78833) from ventricular cardiomyocytes isolated from E14.5 ventricles. *Hcn2-RE1* oligonucleotides (Supplementary Table S1) with methylated non-CpG or CpG sites were labeled with biotin at their 3′-ends

(Integrated DNA Technologies, Inc., Coralville, CA, USA). In the super-shift experiments, the nuclear extracts were pre-incubated with anti-REST antibody (EMD Millipore, 17-641). Protein–DNA binding complexes were separated on a 6% DNA retardation gel, detected using the ECL regent and quantified using the ImageJ software (37).

In vitro DNA methylation assay

Cytosines of the PGL3-enhancer vector with or without the *Hcn2-RE1* were methylated using *SssI* recombinant methyl-transferase (NEB, M0226M). Two microgram of plasmid DNA were incubated with 4 U *SssI* in *t*he presence of 320 µM S-adenosyl methionine for 2 h at 37°C. The reaction was stopped by heating at 65°C for 20 min. The DNA was purified by gel extraction. Methylation of plasmids was verified by bisulfite sequencing.

Immunofluorescence

Primary embryonic and neonatal ventricular cardiomyocytes were seeded onto Matrigel-coated Nunc Thermanox and poly-L-lysine/laminin-coated glass coverslips, transfected with 100 nM siRNA for *Dnmt3a*, *Dnmt3b* or *Rest* by the Lipofectamine LTX and PLUS Reagents for 48 h, and then exposed to anti-HCN2 (Proteintech, 555245-1-AP, 1:500), REST (Antibodies-online, ABIN747683, 1:500) and DNMT3B (Abcam, ab13604, 1:500) antibodies. The samples were detected with Cy3-labeled goat anti-rabbit IgG and counterstained using DAPI. The stained cardiomyocytes were analyzed using a Carl Zeiss imaging system (Thomwood, NY, USA).

RNA sequencing

Ten micrograms of total RNA were extracted from the ventricular tissue of wildtype or myocardial deletion of *Rest* embryos at E12.5 using the miRNeasy Mini kit. Each of the two groups included three biological replicates, pooling four hearts for each replicate. Total RNA was checked for quantity and quality on an Agilent Bioanalyzer 2100, with an RNA Integrity Number (RIN) of ≥8.0. Libraries were prepared according to Illumina TrueSeq RNA library method using the 'TrueSeq RNA Sample preparation guide' (Illumina Technologies). The fragment distribution of libraries was examined on an Agilent High Sensitivity DNA Bio-Analyzer chip, quantified using real-time PCR, and used to prepare clusters using a One-Touch 2 device. These clusters were then sequenced on Illumina HiSeq 2500, to generate 100 bp paired reads.

RNA-seq data analysis

RNA-seq reads were mapped to the mouse reference genome (GRCm38.p4) using TopHat v2.0.13 (38). Based on the GENCODE database (vM6) (39), the number of RNA-seq fragments mapped to each gene was determined by HT-Seq (40). DESeq2 (41) was then used to analyze the fragment counts for identifying differentially expressed genes (DEGs), at a false discovery rate (FDR) <0.05. The gene expression values, measured as Fragments Per Kilobase of

exon per Million fragments mapped (FPKMs), were initially generated by Cufflinks (version 2.2.1) (42). The FP-KMs were converted to transcripts per millions (TPMs) as described previously (43). We restricted our differential expression analysis to the 11 266 protein-coding genes with average TMP >1 in either WT or KO samples. Ingenuity Pathway Analysis (IPA) (http://www.qiagen.com/ingenuity) was used for functional enrichment analysis. The RNA-seq data have been deposited in the GEO (accession number: GSE80378). Using qRT-PCR and qChIP assays, we verified the genes co-regulated and co-occupied by REST and DNMT3B on E12.5 ventricles from either myocardial *Rest* or *Dnmt3b* null embryos. Also, we randomly selected 6 of the 41 REST-targeted genes for non-CpG methylation assay for their RE1 by bisulfite sequencing. The primers for qRT-PCR, qChIP and bisulfite sequencing are listed in Supplemental Tables S2, S3 and S4, respectively.

Identification of REST directly targeted genes

Genome-wide REST binding peaks in the mouse embryonic stem cells were derived from previous work (44). Promoter regions were defined as 5 kb upstream of a transcription start site (TSS) to 1 kb downstream, with distal regulatory regions defined as within the remaining 50 kb of the TSS. Genes with at least one peak in the promoter or distal regulatory regions were defined as REST binding genes.

Developmental expression analysis of REST targets

Microarray data for developing mouse hearts were obtained from a previous meta-analysis (45). Ventricle data were available for E12.5–E18.5 but for not other stages, so we used data from whole hearts for those stages.

Statistical analysis

All *in vitro* experiments were performed as biological triplicates and each sample as technical triplicates. *In vivo* experiments were collected from at least 6 mice of each genotype. Statistical analyses were performed using Student's t test, Mann–Whitney test, Dunnett multiple comparison test, as appropriate (SPSS 16.0 software). Data were presented as mean ± standard deviation (SD), and two-tailed, $P < 0.05$ was considered a significant difference.

RESULTS

Increased *Hcn2* expression in the developing heart is associated with downregulation of DNMT3B and non-CpG methylation of a functional Hcn2-RE1

To determine the expression profile and regulation mechanism of REST-targeted genes during heart development and maturation, we first focused on the genes encoding cardiac ion channels, by testing the expression of the *Hcn1-4* in postnatal day 21 (P21) ventricles using qRT-PCR. The result showed that *Hcn2* was the predominantly expressed channel (Figure 1A). As REST suppresses *Hcn2* transcription through binding to an *Hcn2*-RE1 in intron 1 (5), we then examined the developmental expression profile of *Hcn2* in embryonic hearts by qRT-PCR and Western blot

analyses. We found that *Hcn2* expression was developmentally upregulated from E10.5 to P21 as cardiac ion channels became fully mature (Figure 1B–D). Meanwhile, REST expression was maintained at a consistently high level between E10.5 and P1, but drastically downregulated from P1 to P21.

Since DNMT1 has been suggested to be a potential REST co-factor (12) and DNA methylation at CpG sites of the RE-1 motif has been shown to be overall low and affected by REST occupancy in embryonic stem cells and neural progenitors (44,46,47), we next examined the expression of DNMTs (*Dnmt1*, *Dnmt3A* and *Dnmt3B*) and found that the expression of the DNMT3s, especially DNMT3B, was also downregulated from E10.5 to P1, whereas DNMT1 expression was relatively stable (Figure 1C and D). This promoted us to examine DNA methylation of the *Hcn2*-RE1 by bisulfite sequencing (Figure 1E and F). The results showed that DNA methylation at the non-CpGs was more dynamic than at the CpG site, and the level of DNA methylation at the non-CpGs reduced with progression of heart development (Figure 1G & Supplementary Figure S1), especially from E14.5 (57.9 ± 8.6%) to E18.5 (17.9 ± 1.9%), and a further reduction at P1 (4.8 ± 1.7%). In contrast, the one CpG within the RE1 site and the adjacent CpGs were stably hypomethylated (<5%) throughout development. The findings suggest that non-CpG rather than CpG methylation of the *Hcn2*-RE1 may play a role in *Hcn2* expression during heart development.

Hcn2 silencing in the developing heart depends on the non-CpG methylation of the Hcn2-RE1 by DNMT3B

We next tested whether DNMT3A or DNMT3B is involved in the regulation of *Hcn2*. Chromatin immunoprecipitation (ChIP) and re-ChIP assays showed that REST and DNMT3B, but not DNMT3A, co-occupied the *Hcn2*-RE1 in E14.5 ventricles, reflected by an enrichment of *Hcn2*-RE1 sequence in the immunoprecipitated DNA (Figure 2A). The occupancy of each protein gradually reduced from E14.5 to P1 (Figure 2B). Interestingly, the reduction of their occupancy appeared to follow the trend of decreasing non-CpG methylation in the *Hcn2*-RE1 (Figure 2C). To test whether REST binding and transcriptional repression of *Hcn2* were affected by DNA methylation directly, we generated unmethylated and methylated pGL3 enhancer reporter constructs with or without *Hcn2-RE1*, and quantified reporter luciferase activity in cultured P1 cardiomyocytes. The results showed that a functional *Hcn2*-RE1 is required for suppressing *Hcn2* transcription in the presence of REST, and the DNA methylation of the RE1 sequence augments the suppression (Figure 2D and E). Furthermore, we found that only *Dnmt3b* overexpression in P1 cardiomyocytes was able to augment the REST suppression. While *Dnmt3a* or *Dnmt3b* knockdown by shRNAs had no effect, presumably due to their already very low expression level in cultured P1 cardiomyocytes, overexpression of *Dnmt3b* (but not *Dnmt3a*) increased non-CpG methylation of the *Hcn2*-RE1 (Figure 2F and Supplementary Figure S2). Altogether, these results suggest that inactivation of *Hcn2* transcription in embryonic hearts depends on non-CpG methylation of the *Hcn2*-RE1 by DNMT3B.
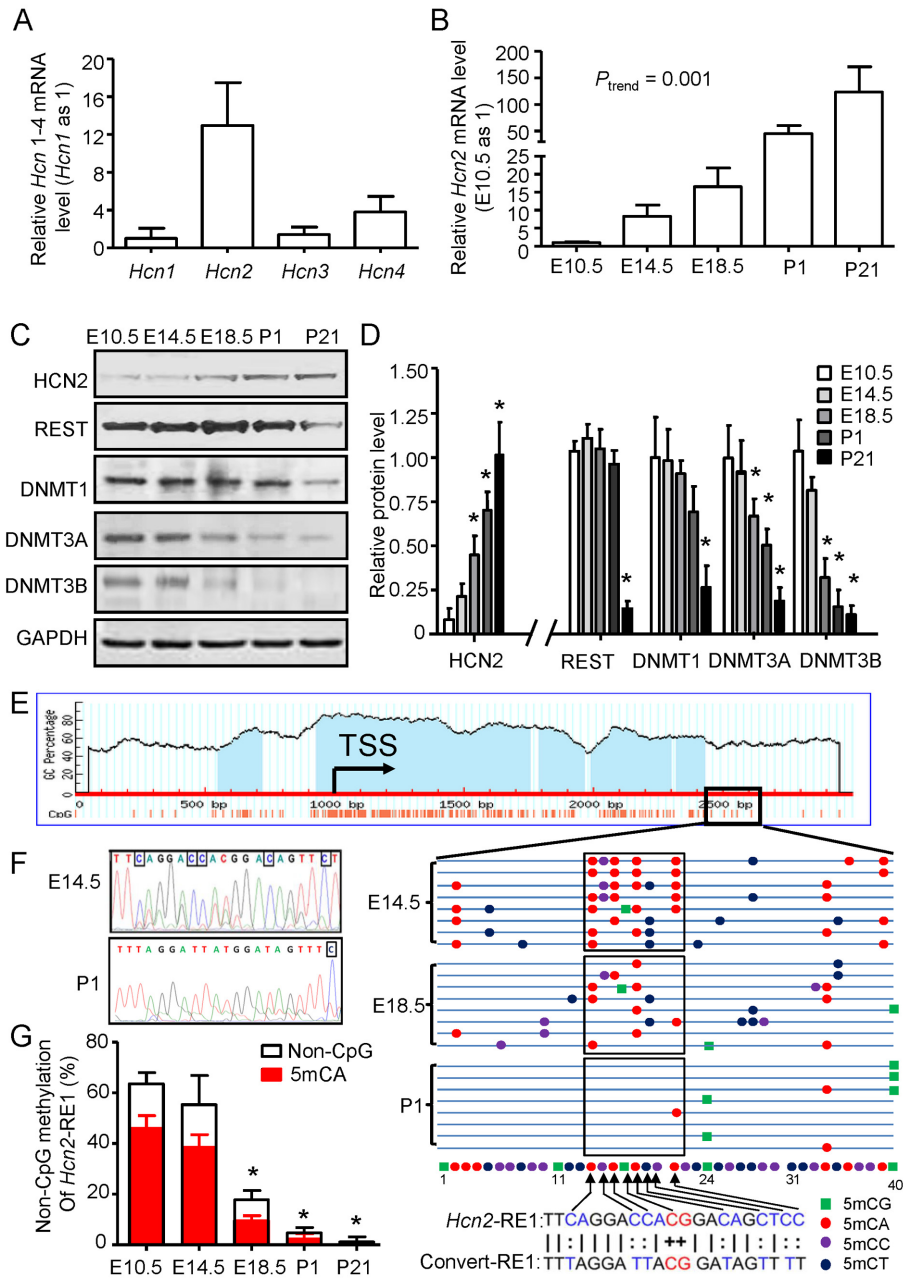
Figure 1. Increased HCN2 expression in developing hearts and its association with decreased REST and DNMT3 expression and reduced non-CpG methylation of an intronic REST binding element in the *Hcn2* gene *(Hcn2-RE1)*. (A, B) qRT-PCR analysis of *Hcn1-4* showed that *Hcn2* was the predominant form expressed in postnatal ventricles at P21 (**A**), and developmentally upregulated from E10.5 to P21 (**B**). *P* trend-value was calculated using Mann–Kendall test. (C, D) Quantitative Western blot analysis showed that a steadily increased HCN2 level in the developing ventricle from E10.5 to P21 was associated with gradually decreased levels of REST, DNMT3A and DNMT3B. Error bars, SD ($n = 3$–5/stage), *$P < 0.05$ as compared to P21 for HCN2, and E10.5 for DNMT1, DNMT3 and REST. (**E**) Top panel: the Methprimer histogram of CpG islands (blue) and CpG dinucleotides (red vertical lines) in the regulatory region of *Hcn2* (TSS, transcription start site). Boxes indicate a segment of *Hcn2-RE1* in the first intron of *Hcn2*. Bottom right panel: Representative bisulfite sequencing of 8 clones from each stage for the *Hcn2-RE1*. Three mouse hearts were analyzed at each stage, with 8 clones selected for bisulfite sequencing for each heart. (**F**) Representative bisulfite sequencing data for *Hcn2-RE1* from E14.5 and P1 ventricles. (**G**) Reduction of non-CpG methylation within the *Hcn2*-RE1 (%) in the developing ventricles from E10.5 to P21. Error bars, SD ($n = 3$/stage), *$P < 0.05$ as compared to E10.5 and calculated by the Student's *t*-test. E, embryonic; P, postnatal.
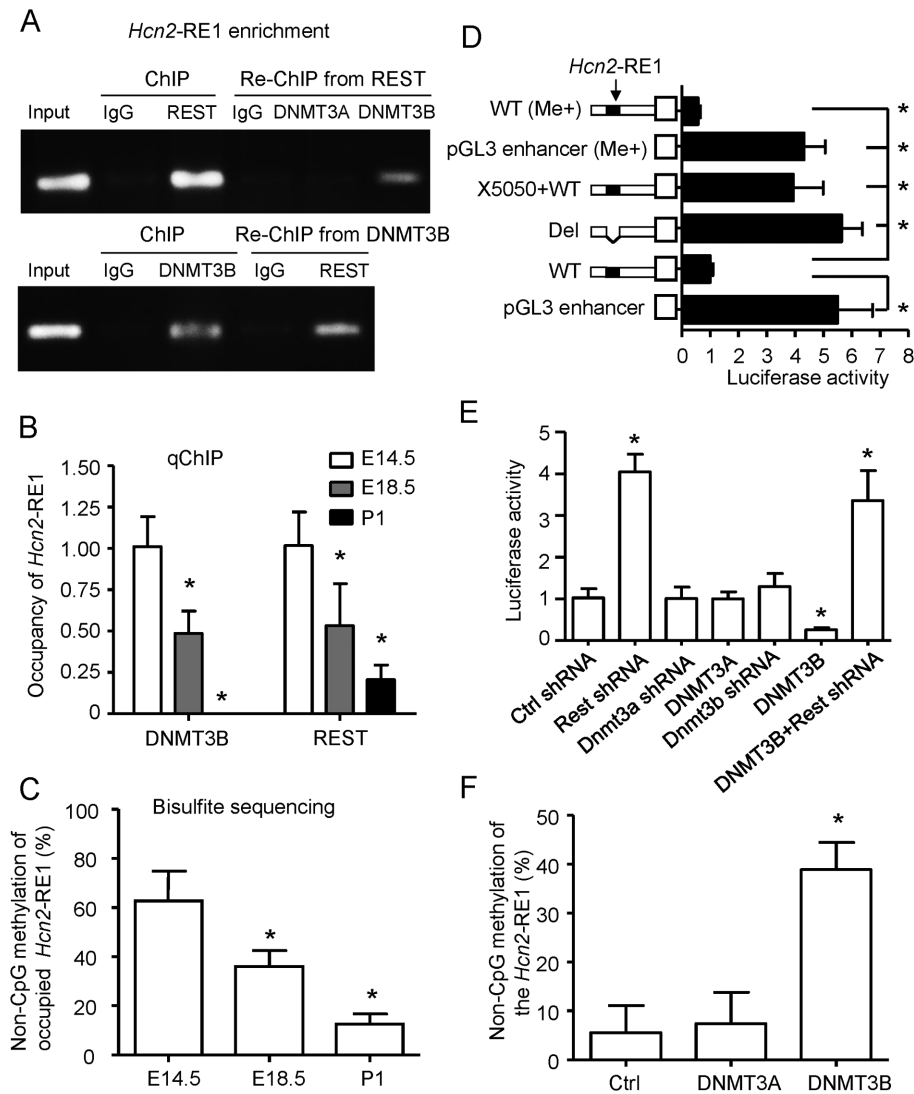
Figure 2. DNMT3B-mediated non-CpG methylation of *Hcn2-RE1* increased REST suppression. (**A**) Enrichment of targeted *Hcn2-RE1* DNA fragments in the chromatin immunoprecipitated by REST and DNMT3A/B antibodies using ChIP and re-ChIP assays and PCR analysis. Top, ChIP by REST and then re-ChIP by DNMT3A, DNMT3B or IgG antibodies (top panel). Bottom, ChIP by DNMT3B and then re-ChIP by REST or IgG antibodies. In all cases, PCR analysis was performed with primers targeting the *Hcn2-RE1* region. Representative images of ChIP and re-ChIP assays showing that the *Hcn2-RE1* is co-occupied by REST and DNMT3B but not DNMT3A in E14.5 ventricles. (**B**) qChIP analyses of the ventricles from E14.5, E18.5 and P1, showing a gradual decrease of DNMT3B and REST occupancy at the *Hcn2-RE1*. (**C**) Quantitative bisulfite sequencing analyses of the *Hcn2-RE1* immunoprecipitated by REST antibody, showing gradually decreasing non-CpG methylation from E14.5, E18.5 and P1. *$P < 0.05$ compared to E14.5. (**D**) Reporter assays using cultured P1 ventricular cardiomyocytes transfected with pGL3 enhancer constructs containing either wild type (WT) or deletion (Del) *Hcn2-RE1* fragment (from bottom to top), showing that the WT *Hcn2-RE1* was required for transcriptional suppression. Reducing REST activities by X5050 abolished the suppression, whereas *in vitro* methylation by *SssI* recombinant methyltransferase of the fragment enhanced its suppression [pGL3 enhancer (Me+) versus WT (Me+)]. (**E**) The shRNA inhibition of *Rest* but not of *Dnmt3a or Dnmt3b* expression increased the transcription of the WT pGL3 enhancer construct, whereas overexpression of *Dnmt3b* but not *Dnmt3a* was repressive. Luciferase activities were measured and normalized to the Renilla activities. *$P < 0.05$ compared to the control pGL3 enhancer construct (D) or scrambled shRNA (Ctrl shRNA) (E). (**F**) Bisulfite sequencing analysis, showing changes in the non-CpG methylation of *Hcn2-RE1* in cultured P1 ventricular cardiomyocytes by overexpression of *Dnmt3a or Dnmt3b*; *$P < 0.05$ compared to the control empty construct (Ctrl). Error bars, SD ($n = 3$–4 independent experiments). *P*-value was calculated using the Student's *t*-test. E, embryonic; P, postnatal.

Non-CpG methylation of the *Hcn2*-RE1 increases REST binding, suppressing *Hcn2* expression

Next, we compared the sequences of the *Hcn2*-RE1 among human, rabbit, rat, and mouse, and found that they share >90% identity. This 21 bp site contains 7 non-CpGs and 1 CpG. We therefore generated *Hcn2*-RE1s with different DNA methylation states of their cytosines and tested their

differences in binding to REST by electrophoretic mobility shift assays (EMSA) using nuclear extracts from E14.5 ventricular cardiomyocytes (Figure 3). The results showed that non-CpG hypermethylation increased REST binding, and that more binding to REST was detected when more non-CpGs were methylated (Figure 3B). In contrast, CpG methylation had zero or limited effect on REST binding. The assay did not test individual Cs, but these results show
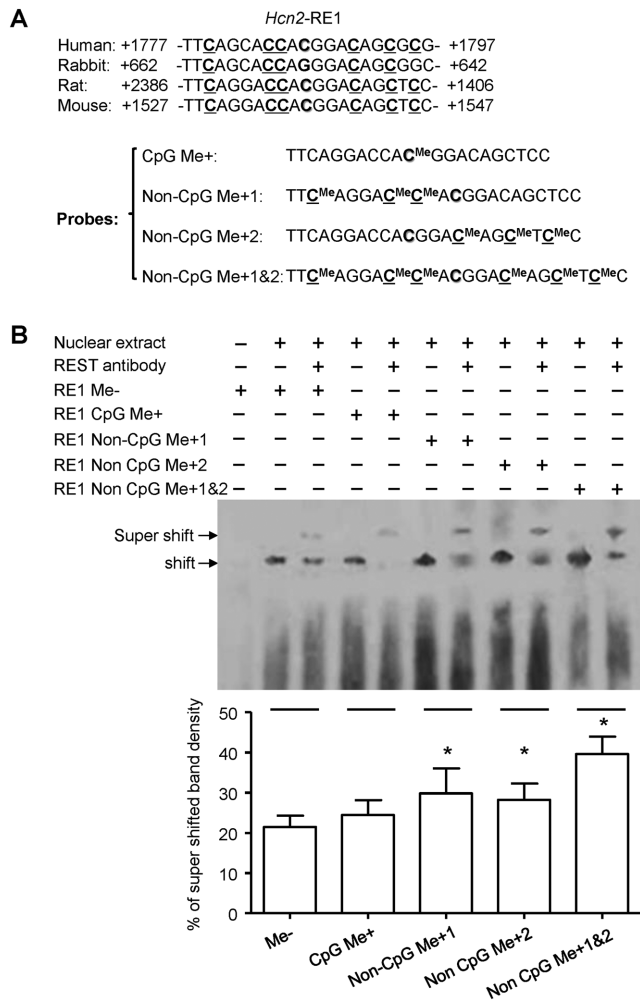
Figure 3. Non-CpG methylation of the *Hcn2-RE1* facilitates REST binding. (**A**) The top panel shows the conservation of the *Hcn2-RE1* among humans, rabbits, and rodents. The bottom panel shows the biotinylated *Hcn2-RE1* with varied CpG or non-CpG methylation (Me+) in probes used for electrophoretic mobility shift assay (EMSA). (**B**) The top panel shows a representative blot of the EMSA assay using nuclear extracts from E14.5 ventricles and the biotinylated *Hcn2-RE1*. The bottom panel shows the percentages (%) of super shifted band / total binding complex, averaged from four independent experiments. Data are presented as mean ± SD, *$P < 0.05$ compared to the unmethylated *Hcn2-RE1* (*Hcn2-RE1* Me-), indicating significantly increased REST binding to the non-CpG methylated *Hcn2-RE1*. *P*-value was calculated using the Student's *t*-test.

that non-CpG methylation at both halves of the *Hcn2*-RE1 facilities REST binding *in vitro*.

Non-CpG methylation by DNMT3B facilitates *Hcn2* suppression by REST

We then directly examined the *in vitro* regulation of *Hcn2* expression by REST and DNMT3B in E14.5 and P1 cardiomyocytes. The results revealed that *Hcn2* transcripts were upregulated by a REST inhibitor (X5050, reducing REST protein level) or *Dnmt3b* knockdown by shRNAs in cultured E14.5 cardiomyocytes, in which there were high levels of REST and DNMT3B (Figure 4A and Supplementary Figure S2A). In comparison, release of *Hcn2* sup-
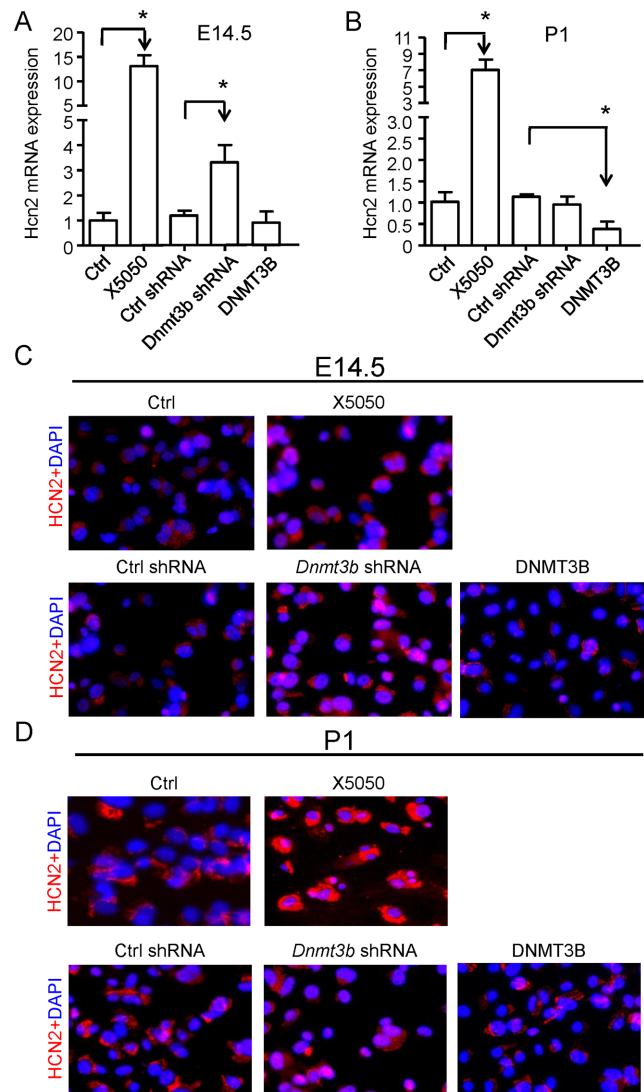

Figure 4. REST and DNMT3B function together to regulate *Hcn2* expression in developing ventricular cardiomyocytes. (**A** and **B**) qRT-PCR analyses showing that *Hcn2* expression in cultured E14.5 or P1 ventricular cardiomyocytes was upregulated by inhibition of REST with X5050. Data are presented as mean ± SD ($n = 4$) *$P < 0.05$ compared to the control without treatment (Ctrl) or scrambled shRNA (Ctrl shRNA). (**C** and **D**) Immunofluorescence confirming that the level of HCN2 proteins (red) in the cultured E14.5 cardiomyocytes was upregulated by X5050, or *Dnmt3b* shRNA, whereas in the cultured P1 cardiomyocytes the HCN2 level was increased by X5050, but decreased by DNMT3B overexpression.

pression by *Dnmt3b* shRNA-mediated knockdown was not seen in cultured P1 cardiomyocytes, in which *Dnmt3b* is expressed at a low baseline level (Figure 4B and Supplementary Figure S2B). Conversely, we found that overexpression of *Dnmt3b* in P1, but not E14.5, cardiomyocytes suppressed *Hcn2* expression. Additionally, we found by immunofluorescence that REST inhibition increased the level of HCN2 in E14.5 cardiomyocytes, whereas overexpression of *Dnmt3b* had no effect at this stage (Figure 4C). In cultured P1 cardiomyocytes, reduction of REST by X5050 or shRNAs increased the level of HCN2, whereas overexpression of *Dnmt3b* reduces its basal expression (Figure 4D).

These observations support the model that *Dnmt3B* down-regulation causes a release of *Hcn2* repression, and non-CpG methylation of the *Hcn2*-RE1 by DNMT3B maintains *Hcn2* repression through increasing or stabilizing REST binding.

Furthermore, we showed by qRT-PCR that in P1 hearts, compared to cardiomyocytes, cardiac fibroblasts expressed a lower level of *Dnmt3a* and *Hcn2* but a higher level of *Dnmt3b* (Supplementary Figure S3A). The same cardiac fibroblast cells were tested by bisulfite sequencing, revealing higher levels of non-CpG methylation of the *Hcn2*-RE1 in comparison to cardiomyocytes (Supplementary Figure S3B). Additionally, expression of *Nppb*, another known REST-targeted gene (5), shared the same patterns of expression and regulation by REST as *Hcn2* (data not shown). Taken together, the results indicate that non-CpG methylation of *Hcn2*-RE1 by DNMT3B facilities *Hcn2* suppression by REST in developing cardiomyocytes. While the suppression is developmentally released in cardiomyocytes, it persists in cardiac fibroblast cells to suppress *Hcn2* expression.

REST and DNMT3B are required for *Hcn2* suppression in embryonic hearts through non-CpG methylation

To confirm the requirement of REST and DNMT3B for regulating myocardial *Hcn2* expression in hearts, we deleted *Dnmt3a, Dnmt3b* and *Rest* individually in the myocardium using the *Troponin T (Tnt)*-Cre transgene (48). The results of Western blot and qRT-PCR analyses showed that these deletions significantly reduced the expression of each of these three genes in the E12.5 ventricle, as expected, and, more importantly, *Dnmt3a, Dnmt3b* and *Rest* deletion resulted in significantly increased *Hcn2* expression (Figure 5A and B). Of note, deletion of *Dnmt3a* or *Dnmt3b* did not affect REST expression. Moreover, qChIP studies and bisulfite sequencing showed that deletion of *Dnmt3b*, but not *Dnmt3a*, reduced non-CpG methylation and REST occupancy at the *Hcn2*-RE1 (Figure 5C and D). qChIP also confirmed that myocardial knockout of *Rest* diminished REST occupancy at the *Hcn2*-RE1, but had no effect on DNMT3B binding (Figure 5E). These observations thus provide strong genetic evidence for supporting the model that non-CpG methylation of the *Hcn2*-RE1 by DNMT3B facilitates REST binding to suppress *Hcn2* transcription during heart development.

Non-CpG methylation at RE1s influences genome-wide REST binding to repress gene expression in the developing heart

To test whether non-CpG methylation of RE1s is required for repression of REST targets other than *Hcn2* in the developing heart, we performed RNA-seq analysis of E12.5 wild type (WT) and *Rest* knockout (KO) ventricles to identify genes repressed by REST, and then investigated whether their expression was also dependent on DNMT3B and non-CpG methylation at their local RE1s. The RNA-seq results showed that the expression levels of 134 genes were significantly REST-dependent (FDR < 0.05) (Figure 6A, **Dataset S1;** GEO:GSE80378). The vast majority (127 of 134, 94.7%) of the differentially expressed genes (DEGs)

were upregulated in the REST-inactivated ventricles, consistent with REST acting as transcriptional repressor. Gene function analysis revealed that REST-suppressed genes in embryonic hearts were enriched for the known functions of REST-targeted genes (11,12,44), including neurotransmission, neuronal development, and seizure-associated properties (Figure 6B). The analysis also found enrichments of DEGs for metal ion transport, cerebrovascular dysfunction, myocardial infarction, cell cycle and ventricular arrhythmia, which are properties related to heart development and function. To demonstrate whether those DEGs are direct REST targets, we used HOMER (49) to analyze transcription factor binding motifs in their promoters and found that the consensus RE1 sequence (Figure 6C) is the only significantly enriched motif, present in 29.4% of the promoters of DEGs, compared with 2.1% of the promoters of non-DEGs (Benjamini corrected $P < 0.0001$, Fisher's test). We then re-analyzed REST ChIP-seq data from the mouse embryonic stem cells (44) and found that our DEGs are significantly more likely to be bound by REST than non-DEGs, both at promoters (odds ratio (OR) = 24.89, $P < 2.2e^{-16}$, Fisher's exact test) and at distal regulation regions (OR = 8.28, $P < 2.2e^{-16}$) (Figure 6D). These results support that the majority of our DEGs are likely to be directly regulated by REST.

DNMT3B and REST co-regulate expression of REST targets in early embryonic hearts

We next identified the genes co-regulated by REST and DNMT3B in the developing heart using qRT-PCR assays on E12.5 ventricles from either myocardial *Rest* or *Dnmt3b* null embryos. Of the 134 DEGs from the RNA-seq results, qRT-PCR confirmed the differential expression of 110 genes (82.1%) in E12.5 myocardial *Rest* null (Figure 6E & Supplementary Table S5) and 77 genes (57.5%) in *Dnmt3b* null ventricles. Together, the results indicate that, of the 110 confirmed REST-suppressed genes, 68 (61.8%) genes were co-regulated by DNMT3B, whereas 42 genes seemed to be regulated by REST only. Of the 68 genes confirmed to have differential expression in both Rest KO and Dnmt3b KO animals, 61 were upregulated in expression (Figure 6E). Of note, each of these 68 co-regulated genes contains one or more putative RE1s that overlap with REST peaks from ChIP-seq data of mouse embryonic stem cells (44). To test the effect of DNMT3B loss on REST occupancy of the RE1s at these 68 co-regulated genes, we performed qChIP and found that in 41 of the 68 genes, REST binding to their putative RE1s was significantly reduced by knockout of *Dnmt3b* but not *Dnmt3a* (Supplementary Table S6). To further test if the non-CpGs in these RE1s were methylated, we randomly selected 6 of the 41 REST/DNMT3B co-targeted genes, including neuronal (*Syn1, Snap25* and *Unc5a*) and cardiac genes (*Nppb, Kcnb1* and *Fgf12*), for bisulfite sequencing analysis of their RE1s and flanking sequences. The results showed that, as with *Hcn2*, non-CpG methylation of the RE1s at these 6 genes was constitutively high in wild type conditions and significantly decreased by the *Dnmt3b* knockout (Figure 6F & Supplementary Table S7). As controls, no changes in DNA methylation were detected for two randomly selected genes (*Mapk8ip1* and *Gabrb3*), whose expression was only dependent on REST
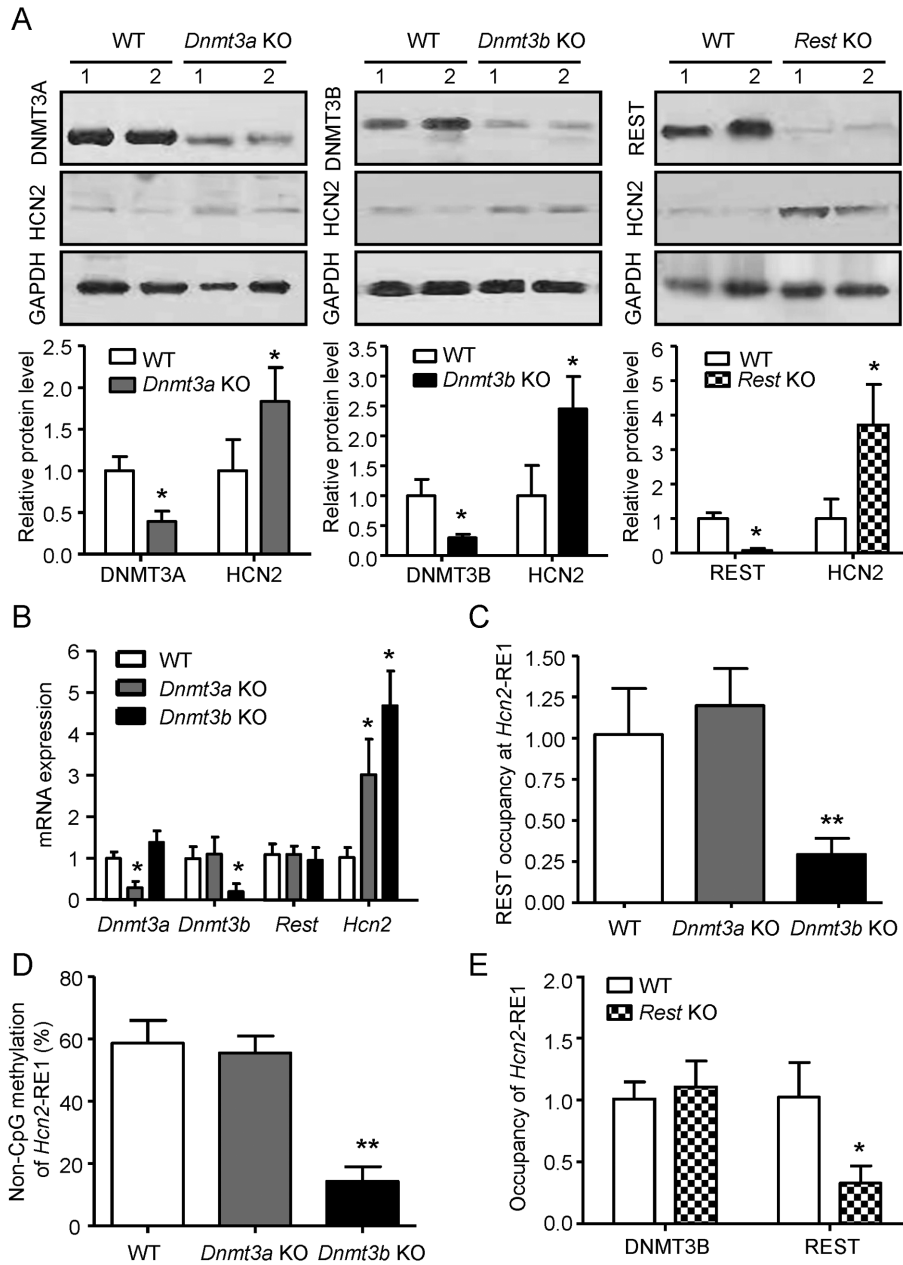
Figure 5. REST and DNMT3B were required for developmentally regulated *Hcn2* expression in the embryonic hearts. (**A**) Western blot analysis showing that the levels of DNMT3A, DNMTB, REST and HCN2 proteins in E12.5 ventricles. Quantification assays indicated that the levels of HCN2 proteins are increased in E12.5 ventricles of myocardial deletion of *Dnm3a* (*Dnmt3a* KO), *Dnmt3b* (Dnmt3b KO) or *Rest* (Rest KO) embryos, *$P < 0.05$ compared to their corresponding wild type (WT) embryos. (**B**) qRT-PCR analysis showing that mRNA expression of *Hcn2*, but not *Rest*, was increased in E12.5 *Dnmt3a* or *Dnmt3b* KO ventricles compared to the WT embryos. (**C**) ChIP-qPCR showing that the occupancy of the *Hcn2-RE1* by REST was decreased in E12.5 by silencing *Dnmt3b*, but not *Dnmt3a*, ventricles. (**D**) Bisulfite sequencing showing a decrease of non-CpG methylation in the *Hcn2-RE1* in E12.5 *Dnmt3b* KO, but not *Dnmt3a* KO, ventricles. (**E**) ChIP-qPCR showing decreased REST occupancy at the *Hcn2-RE1* in E12.5 *Rest* KO ventricles, without any changes in DNMT3B occupancy. *Gapdh* expression was used as an internal control for qPCR and western blot analyses. Data are presented as mean ± SD, $n = 6$ for qPCR and $n = 8$ for bisulfite sequencing analysis. *$P < 0.05$ compared to WT and calculated using the Student's *t*-test.

(Supplementary Figure S4 & Table S7). The results thus indicate that non-CpG methylation of RE1s by DNMT3B is likely to be a general mechanism for regulating a subset of REST targets throughout the mouse genome in the developing heart.

REST and DNMT3B co-regulate temporal gene expression in developing hearts

The above genetic studies compared wild type and mutant embryos at specific time points. To further support that REST and DNMT3B co-regulation has a development role in the dynamic expression of their targets during normal heart maturation, we profiled the developmental expression
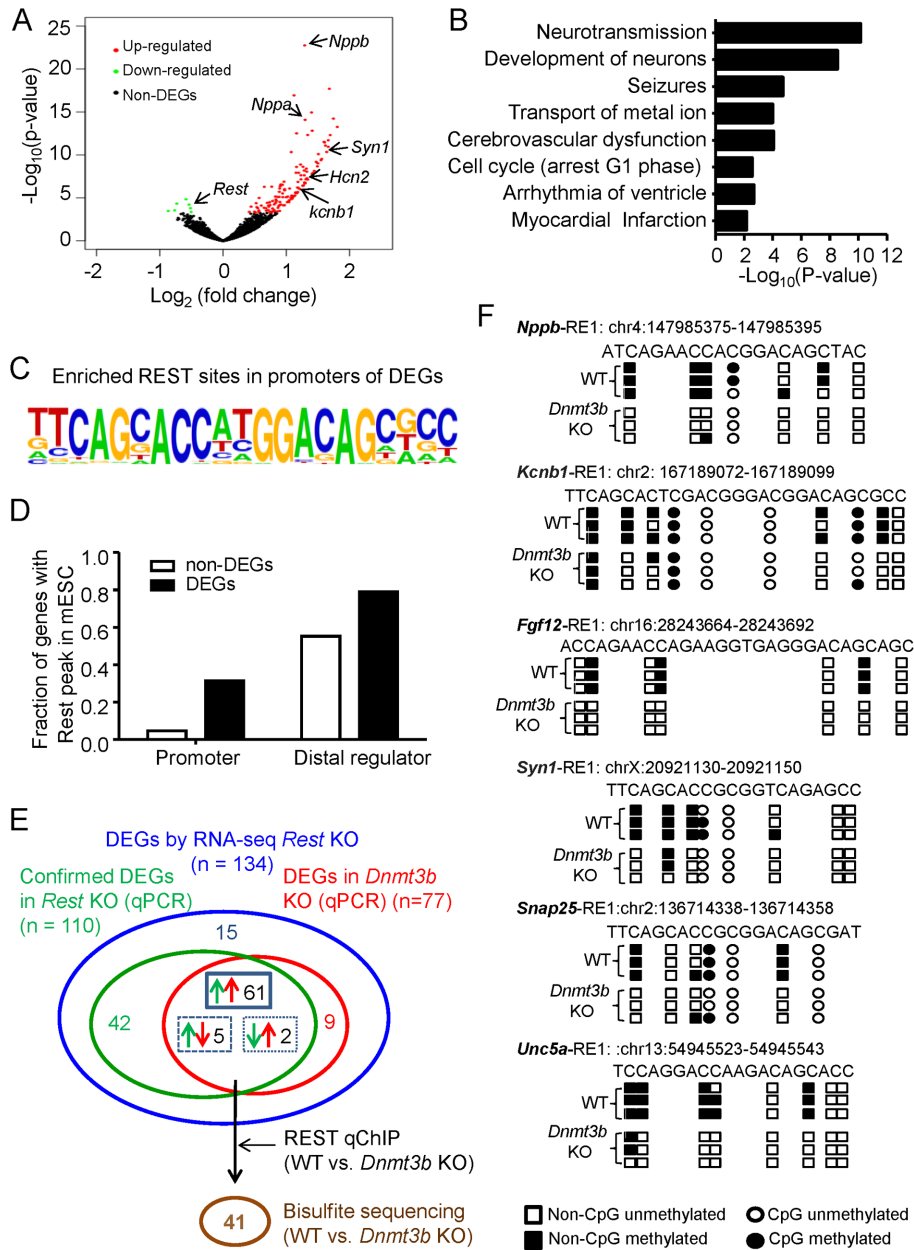
Figure 6. Many REST targets are co-regulated by DNMT3B through non-CpG methylation. (**A**) A volcano plot shows differential gene expression between E12.5 WT and *Rest* KO ventricles. Red and green dots represent significantly upregulated and downregulated genes in the KO, respectively (FDR < 0.05). (**B**) Enriched function terms in differentially expressed genes. (**C**) The only motif enriched in the promoters of DEGs (versus non-DEGs) was the consensus RE1 motif. (**D**) Significantly greater fractions of DEGs contained REST ChIP-seq peaks (from mouse embryonic stem cells, ESCs) in their promoters and distal regulator regions than non-DEGs. (**E**) Diagram showing the procedure and result for identifying the REST-suppressed genes that were also regulated by non-CpG methylation and DNMT3B. ↑ for upregulation, ↓ for downregulation. (**F**) Bisulfite sequencing showing decreased non-CpG methylation of REST sites in all six randomly selected REST/DNMT3 co-regulated genes (from 41 genes) in E12.5 *Dnmt3b* KO ventricles compared with WT ventricles.

of the 110 REST regulated genes (confirmed by qRT-PCR) using microarray data from a previous report (45), which quantified gene expression of mouse hearts (or ventricles) at multiple developmental stages [E10.5, E12.5, E14.5, E16.5, E18.5, P10, P10W (postnatal 10 weeks) and P13W]. Of the 110 genes, 63 were represented in the pre-processed microarray data, including 35 shown to be co-regulated by REST and DNMT3B in our above analysis. As we observed for *Hcn2* (Figure 1), the expression of the majority of the 35

REST and DNMT3B co-regulated genes increased at late gestation, at E18.5 and after birth (Supplementary Figure S5). In contrast, the group of 28 genes whose expression was regulated by REST but not DNMT3B exhibited two patterns, with one cluster (*n* = 11) displaying negative expression correlations (low in early and high in later stages, referred as 'REST only reg-up') and the other (n = 17) positive correlations with *Rest* expression ('REST only reg-down') (Supplementary Figure S5). Examining the average

fold-change (compared with E10.5) at individual stages for the three groups of REST targets (Figure 7A), we found that genes in the 'REST only reg-up' group did not change their expression very much during the prenatal stages (E10.5–E18.5), but were significantly upregulated postnatally from P10, in a trend concurrent with the timing of postnatal downregulation of REST expression (Figure 1), indicating that the expression of these genes is likely to be directly repressed by REST during normal heart development. The expression of the 'REST only reg-down' group, in contrast, decreased their expression gradually from E10.5 to E16.5, but then became stably low up to P13 weeks, suggesting that REST is probably not the major regulator of their expression. More interestingly, for REST and DNMT3B co-regulated genes ('REST and DNMT3B co-reg'), their expression started to increase at the late stages between E16.5 and E18.5, which was coincident with the downregulation of DNMT3B, as determined by western blot analysis (Figure 7B). Their expression then continued to increase by P10, which was again coincident with the downregulation of REST (Figure 7A and B). Note that Rest expression is subject to post-transcriptional regulation (50,51) and therefore protein level is a better approximation of its regulatory function than mRNA abundance. These results suggest that the suppression of the REST/DNMT3B co-regulated targets is released earlier than that of the REST-only targets. Overall, the results support that REST and DNMT3B co-regulate a group of genes during heart development and myocardial maturation, potentially through modulating the DNA methylation levels of the non-CpGs in the REST-binding sites of these genes, thus revealing a critical role of non-CpG methylation in heart maturation (Figure 7C).

DISCUSSION

The current study addresses how REST and DNMT3B function coordinately to suppress the expression of adult genes in early developing mouse hearts and release their repression at a later developmental period. Collectively, our results demonstrate that ∼60% of REST-targeted genes in the embryonic heart are controlled at least partially by DNMT3B. Furthermore, for 41 of these 68 REST target genes, REST occupancy at their RE1s is likely to be facilitated by DNMT3B, whose function appears to involve depositing non-CpG methylation locally. The findings support a previously unappreciated model of REST suppression of gene expression in the developing heart by using both DNMT3B and non-DNMT3B dependent mechanisms, as illustrated in Figure 7C.

Consistent with the observations of higher REST expression during early stages of neuronal differentiation (10), we found that REST is expressed at high levels in developing mouse hearts to repress the cardiac expression of its target gene *Hcn2* prior to E14.5. We found that, despite high levels of REST expression between E18.5 and P1, *Hcn2* expression starts at E12.5 and reaches a sustained high level from P1 onward, indicating that additional levels of regulation exist to allow derepression of REST targets during later cardiac development and maturation (prior to P1). Our study of this derepression points to a role of *Dnmt3b* (but not *Dnmt3a*), as *Dnmt3b* downregulation is associated with ear-

lier increased expression of *Hcn2*. We tested these findings using multiple complementary assays, which revealed that non-CpG methylation of the *Hcn2-RE1* was dependent on DNMT3B, and that DNMT3B promoted REST binding to the *Hcn2-RE1* to suppress *Hcn2* transcription. All together, our findings provide the first evidence that DNMT3B is required for non-CpG methylation at the functional RE1 sequences of essential cardiac genes, which in turn facilitates REST binding and gene repression.

Two research groups have previously examined the relationship between REST binding and DNA methylation. In non-neuronal cells, hypermethylation (in the CpG context) was observed at REST binding sites and the recruitment of DNMT1 by REST was proposed to be a potential cause (10,12). In mouse embryonic stem cells and neuronal stem cells, Schübeler *et al.* found that REST, like CTCF, binds to DNA to create low methylated regions (LMRs), and that *Rest* KO resulted in an increase of local DNA methylation (46,47). Consistent with these findings, we also observed that the CpG in the *Hcn2*-RE1 (Figure 1E) and the RE1s of other REST targets, as well as the CpGs flanking these RE1s exhibited hypomethylation (5∼30%) (Figure 6F & Supplementary Table S3). The CpG methylation flanking the *Hcn2*-RE1 was slightly increased from E12.5 to E18.5 and P1 (Figure 1E). However, we found that non-CpG methylation at RE1s specifically facilitates REST binding to its targets in the developing mouse heart. Since the previous studies did not consider non-CpG methylation, it was not tested whether there is a difference in methylation between non-CpGs and CpGs within RE1s in the stem cells studied. It is nevertheless conceivable that the seemingly discrepancy could be a result of continuous crosstalk between transcription factor binding and local DNA methylation. Putting this in the content of REST function, it is possible that non-CpG methylation facilitates REST binding to RE1 sites, and then DNA methylation in the REST-bound regions may be subsequently increased or decreased in a context-specific manner, depending on whether methyltransferases or demethylases are recruited to or blocked by REST occupancy at individual sites. Consistent with this, 5-hydroxymethlcytosine (5hmC) was found to be enriched at the REST binding site, and *Rest* deletion led to a decrease of 5hmC and a concomitant increase of DNA methylation at the REST binding sites (47). This scenario, however, does not address how DNMT3B is recruited to RE1s for methylating the non-CpGs, a critical question that remains to be addressed in the future. On the other hand, CpA methylation was previously reported to promote Mecp2 (methyl CpG binding protein 2) binding to its targets (52). Our current results show that hypermethylation of non-CpGs (mostly CpAs), known to have a relatively higher affinity for DNMT3B than DNMT3A (53), within RE1s enhances REST binding (Figures 1E–G and 5F). It will therefore be interesting to address in the future whether this dynamic pattern of DNA methylation is different between non-CpG and CpG cytosines in a tissue and/or stage specific manner, and how the DNA methylation changes influence the functions of REST and other transcription factors during development.

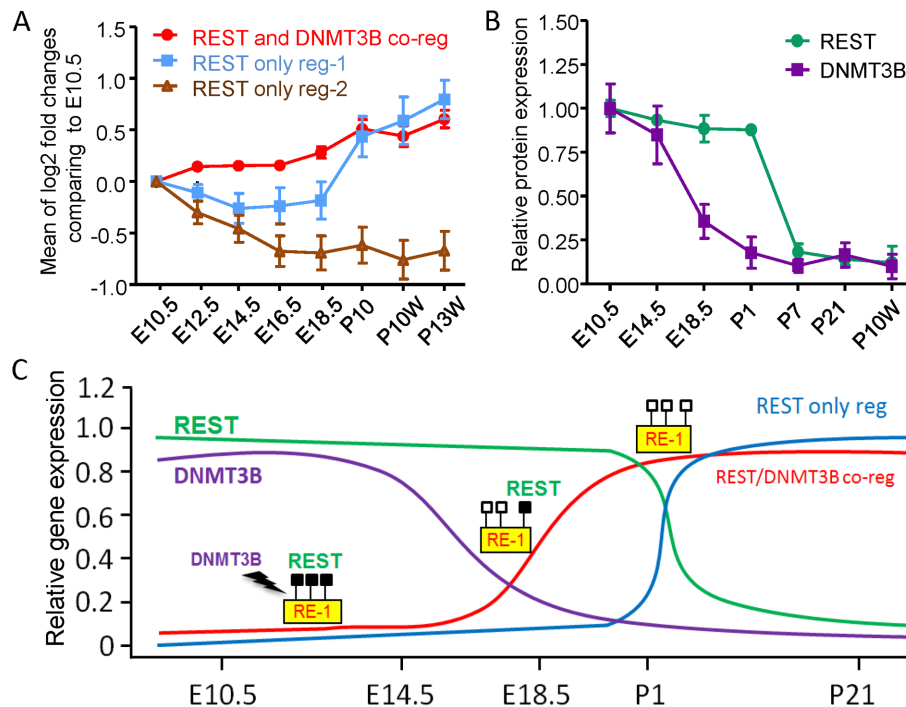Our results indicate that DNMT3B-regulated REST repression plays a critical role in suppressing *Hcn2* transcrip-

Figure 7. Developmental expression profiles of REST and DNMT3B regulated genes in mouse embryonic and adult hearts. (**A**) Average expression changes for the three groups of REST-regulated genes as described in Supplemental Figure S5. For each gene and each stage, expression change was calculated in relation to E10.5 data. The fold changes were averaged within each group and shown on the y-axis as $\log_2$ (fold change) $\pm$ SEM. E12.5 to E18.5 were microarray data for ventricles and the rest were for whole hearts. (**B**) Developmental expression patterns of REST and DNMT3B proteins, as determined by western blot analysis. Data are mean $\pm$ SD ($n = 3$–6 per stage). (**C**) A schematic model showing the activation of REST/DNMT3B co-regulated targets occurs before the activation of genes suppressed by REST only during heart development. Three small boxes are used to depict only the temporal reduction of non-CpG methylation in RE1s of REST targets, and not for illustrating the contribution of any specific non-CpGs.

tion during earlier embryonic heart development, whereas later in development, downregulation of DNMT3B releases such suppression to allow HCN2 to become the major channel expressed in the cardiomyocytes of the mature heart. Therefore, our study reveals a previous unknown developmental and molecular mechanism that drives *Hcn2* transcription to become the primary HCN protein in the adult heart (8). Our genome-wide analysis further showed that many other key genes important for adult heart functions are likely regulated in a manner similar to *Hcn2* by REST and DNMT3B through the dynamic change of non-CG methylation in the RE1s of REST targets. The dynamic interaction between REST binding and DNA methylation is probably critical, as the adult cardiac genes need to be repressed in early embryonic stage but then derepressed later.

Recent genome-wide DNA methylation studies have indicated that non-CpG methylation (mostly in the CpA context, but with contributions from CpTs and CpCs) is abundant in embryonic stem cells, but decreases during tissue development and differentiation (17,27,28), with the exception of tissues like adult brains, in which non-CpG methylation may reach as high as 25% of all cytosine methylation (52,54). Since high expression of DNMT3A and DNMT3B can be associated with high levels of non-CpG methylation (27), and the deletion of *Dnmt3a* and *Dnmt3b* results in hypomethylation of non-CpG cytosines (28), non-CpG methylation has suggested to be mainly controlled by the

activities of DNMT3A and DNMT3B (27,28). This model is consistent with our results.

The functional importance of non-CpG methylation in mammalian cells remains to be fully studied, but evidence for its role in the regulation of several genes has been established. For instance, an increase of non-CpG methylation in the *PPARGC1A* promoter was induced by an exposure of skeletal muscle cells to TNF-alpha or free fatty acids, and associated with the downregulation of *PPARGC1A* expression (54). Likewise, Chen *et al.* (55) showed that non-CpG hypermethylation occurred preferentially in a subgroup of genes (e.g. *Bdnf*) important for brain development, whereas CpG methylation showed relatively less change. MeCP2, a transcription factor whose mutation leads to Rett syndrome, also binds to non-CG (CA) methylated DNA and regulates gene expression as neurons mature (52,55). For developing hearts, Gilsbach *et al.* have recently reported a large number of genomic regions to be differentially DNA methylated during development and maturation of cardiomyocytes (14). In particular, *de novo* methylation by DNMT3A/B causes repression of fetal cardiac genes, whereas demethylation of cardiomyocyte gene bodies is correlated with increased expression during cardiac development (14). In this study, we extend these observations by showing a critical role of non-CpG methylation in the suppression of REST targets in developing hearts.

We have focused here on the roles of DNMT3B and non-CpG methylation in modulating the repression of REST

targets. As shown in Figure 7 and Supplementary Figure S5, the expression of some REST targets identified from our RNA-seq analysis and qRT-PCR validation did not show a negative expression correlation with REST during normal heart development. Some of them are neural genes (e.g. *Ache* and *Nefl*), whose low expression in adult hearts is perhaps repressed by epigenetic mechanisms that involve REST only in early developmental stages, as previously proposed (10). Interestingly, a few genes exhibit a bimodal expression pattern, with high expression in both early embryonic and adult hearts. It is, however, unclear whether this is related to functional importance of those genes in two developmental stages. As we used microarray data from previous publication (45), which itself was derived from multiple studies using different platforms, tissues or cells, these results need more careful follow-up studies, including the seeming difference between P10D and P13W expression for several REST targets.

In summary, our study highlights a new paradigm of transcriptional regulation critical for cardiac development and maturation that is controlled by the interaction of REST, DNMT3B and non-CpG methylation. As disruptions of the normal temporal expression of cardiac genes during development underlie a number of heart diseases, our findings provide new insights into potential mechanisms that can lead to the disruptions.

SUPPLEMENTARY DATA

Supplementary Data are available at NAR Online.

ACKNOWLEDGEMENTS

FUNDING

REFERENCES

1. Rizki,G. and Boyer,L.A. (2015) Lncing epigenetic control of transcription to cardiovascular development and disease. *Circ. Res.*, **117**, 192–206.
2. Li,Y., Klena,N.T., Gabriel,G.C., Liu,X., Kim,A.J., Lemke,K., Chen,Y., Chatterjee,B., Devine,W., Damerla,R.R. *et al.* (2015) Global genetic analysis in mice unveils central role for cilia in congenital heart disease. *Nature*, **521**, 520–524.
3. Chen,Z.F., Paquette,A.J. and Anderson,D.J. (1998) NRSF/REST is required in vivo for repression of multiple neuronal target genes during embryogenesis. *Nat. Genet.*, **20**, 136–142.
4. Chong,J.A., Tapia-Ramirez,J., Kim,S., Toledo-Aral,J.J., Zheng,Y., Boutros,M.C., Altshuller,Y.M., Frohman,M.A., Kraner,S.D. and Mandel,G. (1995) REST: a mammalian silencer protein that restricts sodium channel gene expression to neurons. *Cell*, **80**, 949–957.
5. Kuwahara,K., Saito,Y., Takano,M., Arai,Y., Yasuno,S., Nakagawa,Y., Takahashi,N., Adachi,Y., Takemura,G., Horie,M. *et al.* (2003) NRSF regulates the fetal cardiac gene program and maintains normal cardiac structure and function. *EMBO J.*, **22**, 6310–6321.
6. Kuwahara,K. (2013) Role of NRSF/REST in the regulation of cardiac gene expression and function. *Circ. J.*, **77**, 2682–2686.
7. Bucchi,A., Barbuti,A., Difrancesco,D. and Baruscotti,M. (2012) Funny current and cardiac rhythm: insights from HCN knockout and transgenic mouse models. *Front. Physiol.*, **3**, 240.
8. Herrmann,S., Layh,B. and Ludwig,A. (2011) Novel insights into the distribution of cardiac HCN channels: an expression study in the mouse heart. *J. Mol. Cell. Cardiol.*, **51**, 997–1006.
9. Huang,X., Yang,P., Du,Y., Zhang,J. and Ma,A. (2007) Age-related down-regulation of HCN channels in rat sinoatrial node. *Basic Res. Cardiol.*, **102**, 429–435.
10. Ballas,N., Grunseich,C., Lu,D.D., Speh,J.C. and Mandel,G. (2005) REST and its corepressors mediate plasticity of neuronal gene chromatin throughout neurogenesis. *Cell*, **121**, 645–657.
11. Rockowitz,S., Lien,W.H., Pedrosa,E., Wei,G., Lin,M., Zhao,K., Lachman,H.M., Fuchs,E. and Zheng,D. (2014) Comparison of REST cistromes across human cell types reveals common and context-specific functions. *PLoS Comput. Biol.*, **10**, e1003671.
12. Ballas,N. and Mandel,G. (2005) The many faces of REST oversee epigenetic programming of neuronal genes. *Curr. Opin. Neurobiol.*, **15**, 500–506.
13. Chamberlain,A.A., Lin,M., Lister,R.L., Maslov,A.A., Wang,Y., Suzuki,M., Wu,B., Greally,J.M., Zheng,D. and Zhou,B. (2014) DNA methylation is developmentally regulated for genes essential for cardiogenesis. *J. Am. Heart Assoc.*, **3**, e000976.
14. Gilsbach,R., Preissl,S., Gruning,B.A., Schnick,T., Burger,L., Benes,V., Wurch,A., Bonisch,U., Gunther,S., Backofen,R. *et al.* (2014) Dynamic DNA methylation orchestrates cardiomyocyte development, maturation and disease. *Nat. Commun.*, **5**, 5288.
15. Gu,Y., Liu,G.H., Plongthongkum,N., Benner,C., Yi,F., Qu,J., Suzuki,K., Yang,J., Zhang,W., Li,M. *et al.* (2014) Global DNA methylation and transcriptional analyses of human ESC-derived cardiomyocytes. *Protein Cell*, **5**, 59–68.
16. Patil,V., Ward,R.L. and Hesson,L.B. (2014) The evidence for functional non-CpG methylation in mammalian cells. *Epigenetics*, **9**, 823–828.
17. Laurent,L., Wong,E., Li,G., Huynh,T., Tsirigos,A., Ong,C.T., Low,H.M., Kin Sung,K.W., Rigoutsos,I., Loring,J. *et al.* (2010) Dynamic changes in the human methylome during differentiation. *Genome Res.*, **20**, 320–331.
18. Lister,R., Pelizzola,M., Kida,Y.S., Hawkins,R.D., Nery,J.R., Hon,G., Antosiewicz-Bourget,J., O'Malley,R., Castanon,R., Klugman,S. *et al.* (2011) Hotspots of aberrant epigenomic reprogramming in human induced pluripotent stem cells. *Nature*, **471**, 68–73.
19. Lister,R., Pelizzola,M., Dowen,R.H., Hawkins,R.D., Hon,G., Tonti-Filippini,J., Nery,J.R., Lee,L., Ye,Z., Ngo,Q.M. *et al.* (2009) Human DNA methylomes at base resolution show widespread epigenomic differences. *Nature*, **462**, 315–322.
20. Ramsahoye,B.H., Biniszkiewicz,D., Lyko,F., Clark,V., Bird,A.P. and Jaenisch,R. (2000) Non-CpG methylation is prevalent in embryonic stem cells and may be mediated by DNA methyltransferase 3a. *Proc. Natl. Acad. Sci. U.S.A.*, **97**, 5237–5242.
21. Ichiyanagi,T., Ichiyanagi,K., Miyake,M. and Sasaki,H. (2013) Accumulation and loss of asymmetric non-CpG methylation during male germ-cell development. *Nucleic Acids Res.*, **41**, 738–745.
22. Sharma,G., Upadhyay,S., Srilalitha,M., Nandicoori,V.K. and Khosla,S. (2015) The interaction of mycobacterial protein Rv2966c with host chromatin is mediated through non-CpG methylation and histone H3/H4 binding. *Nucleic Acids Res.*, **43**, 3922–3937.
23. Lister,R., Mukamel,E.A., Nery,J.R., Urich,M., Puddifoot,C.A., Johnson,N.D., Lucero,J., Huang,Y., Dwork,A.J., Schultz,M.D. *et al.* (2013) Global epigenomic reconfiguration during mammalian brain development. *Science*, **341**, 1237905.
24. Guo,J.U., Su,Y., Shin,J.H., Shin,J., Li,H., Xie,B., Zhong,C., Hu,S., Le,T., Fan,G. *et al.* (2014) Distribution, recognition and regulation of non-CpG methylation in the adult mammalian brain. *Nat. Neurosci.*, **17**, 215–222.
25. He,Y. and Ecker,J.R. (2015) Non-CG methylation in the human genome. *Annu. Rev. Genomics Hum. Genet.*, **16**, 55–77.
26. Tiedemann,R.L., Putiri,E.L., Lee,J.H., Hlady,R.A., Kashiwagi,K., Ordog,T., Zhang,Z., Liu,C., Choi,J.H. and Robertson,K.D. (2014) Acute depletion redefines the division of labor among DNA methyltransferases in methylating the human genome. *Cell Rep.*, **9**, 1554–1566.

27. Arand,J., Spieler,D., Karius,T., Branco,M.R., Meilinger,D., Meissner,A., Jenuwein,T., Xu,G., Leonhardt,H., Wolf,V. *et al.* (2012) In vivo control of CpG and non-CpG DNA methylation by DNA methyltransferases. *PLoS Genet.*, **8**, e1002750.

28. Ziller,M.J., Muller,F., Liao,J., Zhang,Y., Gu,H., Bock,C., Boyle,P., Epstein,C.B., Bernstein,B.E., Lengauer,T. *et al.* (2011) Genomic distribution and inter-sample variation of non-CpG methylation across human cell types. *PLoS Genet.*, **7**, e1002389.

29. Kaneda,M., Okano,M., Hata,K., Sado,T., Tsujimoto,N., Li,E. and Sasaki,H. (2004) Essential role for de novo DNA methyltransferase Dnmt3a in paternal and maternal imprinting. *Nature*, **429**, 900–903.

30. Nechiporuk,T., McGann,J., Mullendorff,K., Hsieh,J., Wurst,W., Floss,T. and Mandel,G. (2016) The REST remodeling complex protects genomic integrity during embryonic neurogenesis. *eLife*, **5**, e09584.

31. Jiao,K., Kulessa,H., Tompkins,K., Zhou,Y., Batts,L., Baldwin,H.S. and Hogan,B.L. (2003) An essential role of Bmp4 in the atrioventricular septation of the mouse heart. *Genes Dev.*, **17**, 2362–2367.

32. O'Connell,T.D., Rodrigo,M.C. and Simpson,P.C. (2007) Isolation and culture of adult mouse cardiac myocytes. *Methods Mol. Biol.*, **357**, 271–296.

33. Zhang,D., Xie,X., Chen,Y., Hammock,B.D., Kong,W. and Zhu,Y. (2012) Homocysteine upregulates soluble epoxide hydrolase in vascular endothelium in vitro and in vivo. *Circ. Res.*, **110**, 808–817.

34. Zhang,D., Chen,Y., Xie,X., Liu,J., Wang,Q., Kong,W. and Zhu,Y. (2012) Homocysteine activates vascular smooth muscle cells by DNA demethylation of platelet-derived growth factor in endothelial cells. *J. Mol. Cell. Cardiol.*, **53**, 487–496.

35. Li,H., Rauch,T., Chen,Z.X., Szabo,P.E., Riggs,A.D. and Pfeifer,G.P. (2006) The histone methyltransferase SETDB1 and the DNA methyltransferase DNMT3A interact directly and localize to promoters silenced in cancer cells. *J. Biol. Chem.*, **281**, 19489–19500.

36. Chen,Z.X., Mann,J.R., Hsieh,C.L., Riggs,A.D. and Chedin,F. (2005) Physical and functional interactions between the human DNMT3L protein and members of the de novo methyltransferase family. *J. Cell. Biochem.*, **95**, 902–917.

37. Zhang,D., Sun,X., Liu,J., Xie,X., Cui,W. and Zhu,Y. (2015) Homocysteine accelerates senescence of endothelial cells via DNA hypomethylation of human telomerase reverse transcriptase. *Arterioscler. Thromb. Vasc. Biol.*, **35**, 71–78.

38. Kim,D., Pertea,G., Trapnell,C., Pimentel,H., Kelley,R. and Salzberg,S.L. (2013) TopHat2: accurate alignment of transcriptomes in the presence of insertions, deletions and gene fusions. *Genome Biol.*, **14**, R36.

39. Harrow,J., Frankish,A., Gonzalez,J.M., Tapanari,E., Diekhans,M., Kokocinski,F., Aken,B.L., Barrell,D., Zadissa,A., Searle,S. *et al.* (2012) GENCODE: the reference human genome annotation for The ENCODE Project. *Genome Res.*, **22**, 1760–1774.

40. Anders,S., Pyl,P.T. and Huber,W. (2015) HTSeq—a Python framework to work with high-throughput sequencing data. *Bioinformatics*, **31**, 166–169.

41. Love,M.I., Huber,W. and Anders,S. (2014) Moderated estimation of fold change and dispersion for RNA-seq data with DESeq2. *Genome Biol.*, **15**, 550.

42. Trapnell,C., Roberts,A., Goff,L., Pertea,G., Kim,D., Kelley,D.R., Pimentel,H., Salzberg,S.L., Rinn,J.L. and Pachter,L. (2012) Differential gene and transcript expression analysis of RNA-seq experiments with TopHat and Cufflinks. *Nat. Protoc.*, **7**, 562–578.

43. Li,B., Ruotti,V., Stewart,R.M., Thomson,J.A. and Dewey,C.N. (2010) RNA-Seq gene expression estimation with read mapping uncertainty. *Bioinformatics*, **26**, 493–500.

44. Rockowitz,S. and Zheng,D. (2015) Significant expansion of the REST/NRSF cistrome in human versus mouse embryonic stem cells: potential implications for neural development. *Nucleic Acids Res.*, **43**, 5730–5743.

45. Chen,H. and VanBuren,V. (2014) A provisional gene regulatory atlas for mouse heart development. *PLoS One*, **9**, e83364.

46. Stadler,M.B., Murr,R., Burger,L., Ivanek,R., Lienert,F., Scholer,A., van Nimwegen,E., Wirbelauer,C., Oakeley,E.J., Gaidatzis,D. *et al.* (2011) DNA-binding factors shape the mouse methylome at distal regulatory regions. *Nature*, **480**, 490–495.

47. Feldmann,A., Ivanek,R., Murr,R., Gaidatzis,D., Burger,L. and Schubeler,D. (2013) Transcription factor occupancy can mediate active turnover of DNA methylation at regulatory regions. *PLoS Genet.*, **9**, e1003994.

48. Wang,Q., Reiter,R.S., Huang,Q.Q., Jin,J.P. and Lin,J.J. (2001) Comparative studies on the expression patterns of three troponin T genes during mouse development. *Anat. Rec.*, **263**, 72–84.

49. Heinz,S., Benner,C., Spann,N., Bertolino,E., Lin,Y.C., Laslo,P., Cheng,J.X., Murre,C., Singh,H. and Glass,C.K. (2010) Simple combinations of lineage-determining transcription factors prime cis-regulatory elements required for macrophage and B cell identities. *Mol. Cell*, **38**, 576–589.

50. Westbrook,T.F., Hu,G., Ang,X.L., Mulligan,P., Pavlova,N.N., Liang,A., Leng,Y., Maehr,R., Shi,Y., Harper,J.W. *et al.* (2008) SCFbeta-TRCP controls oncogenic transformation and neural differentiation through REST degradation. *Nature*, **452**, 370–374.

51. Guardavaccaro,D., Frescas,D., Dorrello,N.V., Peschiaroli,A., Multani,A.S., Cardozo,T., Lasorella,A., Iavarone,A., Chang,S., Hernando,E. *et al.* (2008) Control of chromosome stability by the beta-TrCP-REST-Mad2 axis. *Nature*, **452**, 365–369.

52. Gabel,H.W., Kinde,B., Stroud,H., Gilbert,C.S., Harmin,D.A., Kastan,N.R., Hemberg,M., Ebert,D.H. and Greenberg,M.E. (2015) Disruption of DNA-methylation-dependent long gene repression in Rett syndrome. *Nature*, **522**, 89–93.

53. Aoki,A., Suetake,I., Miyagawa,J., Fujio,T., Chijiwa,T., Sasaki,H. and Tajima,S. (2001) Enzymatic properties of de novo-type mouse DNA (cytosine-5) methyltransferases. *Nucleic Acids Res.*, **29**, 3506–3512.

54. Barres,R., Osler,M.E., Yan,J., Rune,A., Fritz,T., Caidahl,K., Krook,A. and Zierath,J.R. (2009) Non-CpG methylation of the PGC-1alpha promoter through DNMT3B controls mitochondrial density. *Cell Metab.*, **10**, 189–198.

55. Chen,L., Chen,K., Lavery,L.A., Baker,S.A., Shaw,C.A., Li,W. and Zoghbi,H.Y. (2015) MeCP2 binds to non-CG methylated DNA as neurons mature, influencing transcription and the timing of onset for Rett syndrome. *Proc. Natl. Acad. Sci. U.S.A.*, **112**, 5509–5514.